Modeling Streak Camera Sweep Speeds

M. Fiedler

LABORATORY FOR LASER ENERGETICS
University of Rochester
250 East River Road
Rochester, NY 14623-1299

Abstract

On the OMEGA laser system at the University of Rochester's Laboratory for Laser Energetics (LLE), six P510 streak cameras measure the pulse shape of the 60 OMEGA beam lines. These cameras use a photocathode to convert an optical signal into an electron beam. A voltage ramp then sweeps this electron beam across a phosphor screen which is in turn imaged by a CCD. Currently, 120 images of an eight-pulse fiducial laser with a period of 548 ps are used to obtain approximately 700 measurements of the speed at which the electron beam sweeps across the image (sweep speed). A spline interpolation is then used to obtain sweep speed values at all points on the CCD. Unfortunately, this introduces noise, and fails when the sweep window changes due to unexpected variations in the camera's voltages. In order to deal with these issues, a model was constructed using frequencies obtained from a PSPICE simulation of the camera's sweep circuitry. This model will replace the spline interpolation, yielding a more accurate sweep and allowing data recovery in case of malfunction.

Introduction

Streak cameras are instruments which convert optical signals into images where time is mapped to spatial displacement. They are extremely useful in measuring many types of short duration optical phenomena.[1] As a result, their uses are extremely varied. Their basic construction, however, is largely the same regardless of their use.

First, a photocathode is exposed to the optical signal to be measured, causing the photocathode to emit a beam of electrons (see fig. 1). The number of electrons emitted is proportional to the intensity of the input signal. This electron beam is then accelerated through a potential difference and focused between two plates which have a changing voltage across them. This changing voltage has the effect of changing the electron beam's deflection over time. Finally, at the end of the system, the electron beam impacts on a phosphor screen which fluoresces. The fluorescence is then imaged onto some medium.

The image created has two special characteristics. First, movement across the image represents a change in time, a reflection of the fact that the electron beam moved across the phosphor screen during the exposure. Second,
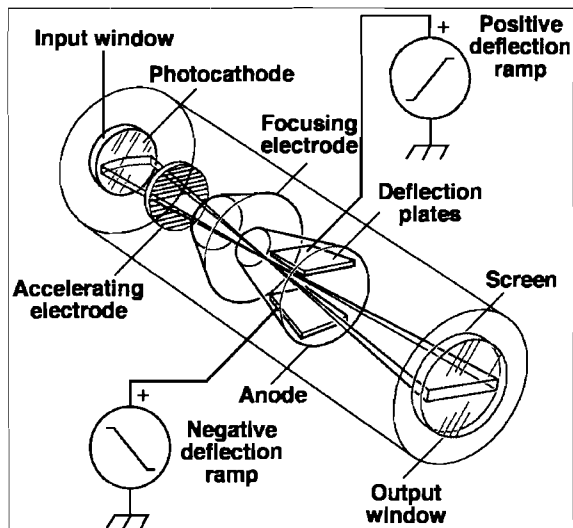

Figure 1

Streak tubes use changing voltages to sweep an electron beam across a phosphor screen over time.

the intensity of the image at a given location is proportional to the intensity of the input signal at the moment in time which corresponds to that image location. This happens because a stronger optical signal causes more electrons to be emitted by the photocathode and thus stronger fluorescence.[1]

Interpreting the image requires that the mapping between time and displacement (the image's time axis) be known. In addition, it is necessary to know the rate at which the electron beam is moving (the sweep speed) at all points in the image in order to normalize the image intensities (i.e. account for the fact that certain parts of the image were exposed for longer periods of time). On most cameras some sort of pulsed, fixed-period laser is used to approximate the time axis and sweep speed. The exact way in which this is done varies from camera to camera.[1]

This work was conducted at the University of Rochester's Laboratory for Laser Energetics (LLE). The lab's main focus is using the 60 beam OMEGA laser system for direct-drive inertial confinement fusion experiments. Such experiments involve hitting a deuterium-tritium target with lasers arrayed in a spherical configuration.[2] At LLE, six P510 streak cameras (all built at LLE) are used to measure the pulse shapes of each of the 60 OMEGA beam lines (ten beams in each camera) as shown in Fig. 3. This data can then be used for power balancing the OMEGA system (i.e. adjusting the laser system in order to improve irradiation uniformity). Better power balance improves the efficiency of inertial confinement fusion.[3] All work for this project was done using P510 cameras. Different types of streak cameras are also used a variety of other purposes at LLE; however, these cameras are not as well calibrated.[4]

Two pieces of software were used during this project. All analysis of P510 data was done using PV-WAVE, a language developed by Visual Numerics. Output from P510's can easily be loaded and manipulated in PV-WAVE using routines developed at LLE. In addition, PSPICE, developed by Cadence Design Systems, was used for circuit simulations.

P510 Characteristics

Each P510 camera receives twelve fiber-optic feeds onto its photocathode and is capable of simultaneously collecting data on all twelve feeds (see fig. 2). Ten of these feeds are hooked up to OMEGA beam lines. The other two are connected to a fiducial timing laser. A CCD
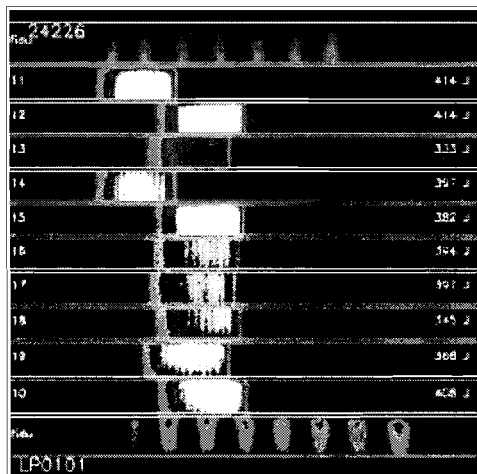

Figure 2

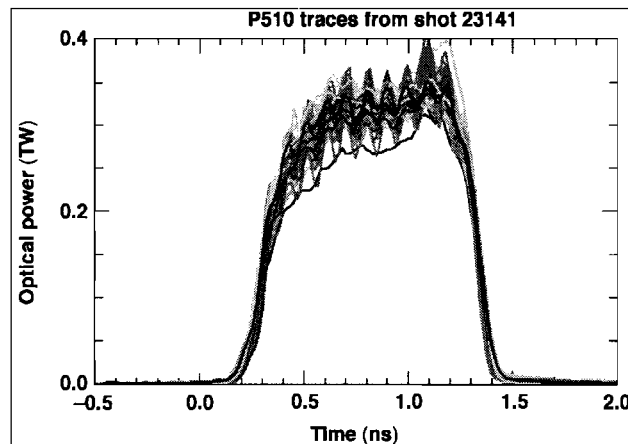P510's produce images with 12 different channels.

Figure 3

Image intensity is used to produce measurements of the beam's optical power with respect to time. This graph shows measurements of the 60 OMEGA beam lines collected using all six P510 cameras.

configured to produce a 512 x 512 image serves as the output device.[3]

One problem with P510 streak cameras is that their voltages drift significantly on a weekly time scale. In order to make measurements at the desired level of a couple percent uncertainty, they must be calibrated weekly. Since the cameras were built at LLE, the calibration routines had to be developed at LLE. This calibration procedure is a three step process. First, geometric distortions resulting from imperfections in the camera's electron optics are corrected by projecting a regular pattern of rectangles through the camera and calculating the distortions in that regular pattern. These distortions can then be undone in the images the camera outputs. Next, the camera is flat fielded in order to compensate for variations in the relative sensitivity of the part of the system which maps to each pixel. This is done by exposing all parts of the system to a light source of uniform intensity for an identical amount of time. Finally, the sweep speed calibration is done, allowing calibration of the time axis and calculation of the electron beam's dwell time on each pixel.[3]

In order to do the sweep speed calibration, an eight-pulse fiducial laser is fed into all twelve channels of the streak camera. As result of the way it is configured, the fiducial has a period of 548 ps. In order to obtain data at as many locations as possible on the CCD, the camera's trigger settings are incremented in order to gradually move the fiducial train across the image. In total, approximately120 images like those in Fig. 4 are taken with the fiducials at different locations in the image. These images are analyzed by calculating the number of pixels between each fiducial peak and then dividing by the time between peaks (the fiducial period of 548 ps). The resulting approximation of the derivative dx/dt is then assigned to the pixel midway between the peaks. From 120 images, this method yields 700 approximations of the sweep speed for each channel. Since any given calibration run does not calculate a value of dx/dt at every pixel across the CCD, a spline interpolation is used to calculate values at every pixel. The time axis can then be generated by integrating this data.[3]
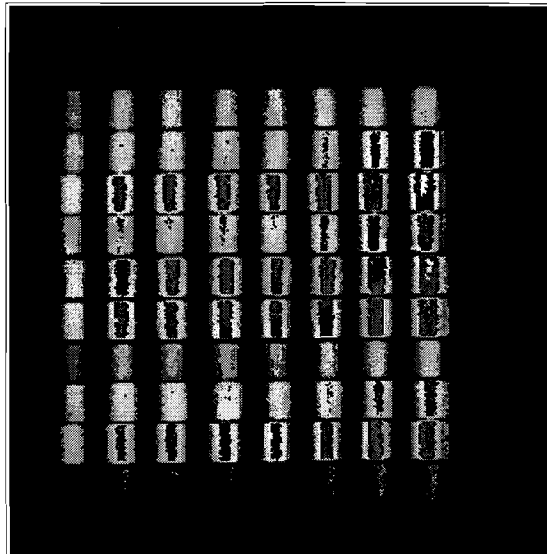
Figure 2

Sweep speed calibration uses 120 images like these in order to calibrate each of the twelve channels.

Unfortunately, this routine has some significant limitations. First, the method for obtaining the sweep speed approximation breaks down at the edges of the image. Once a fiducial pulse gets within 548 ps of the edge of the CCD, the pulse immediately preceding or following it (depending on which edge of the image is involved) does not show up in the image. The result is that sweep speed measurements cannot be obtained within 548 ps of the image's edge (approximately 50 pixels) since there is no second pulse to compare against. This causes the interpolation routine to fail near the edges since it cannot interpolate if no data is available for those portions of the sweep. Another significant limitation is that the data collected is applicable only over the narrow window where the camera is calibrated each week. Unfortunately, during OMEGA shots, the camera's voltages sometimes vary significantly from the set values. The result is a sweep speed different from the one measured during the calibration routine, thus decreasing the accuracy with which the camera's output can be interpreted (see fig. 5). In addition, the
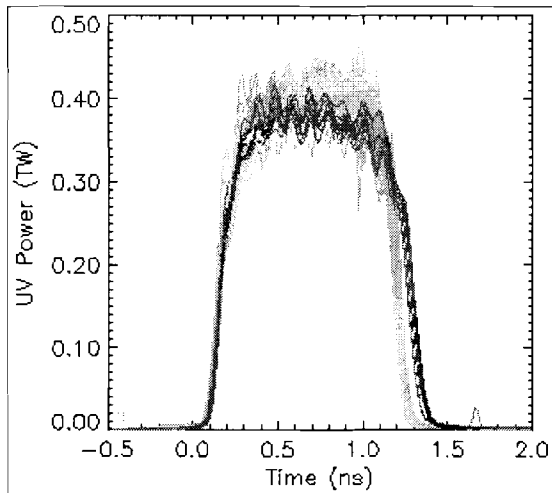
Figure 3

On this OMEGA system shot, one of the six P510 streak cameras malfunctioned and was operating outside of the window for which it was calibrated. As a result, the data obtained on ten of the beam lines have improperly calibrated time axes and do deviate significantly from the other beam lines.
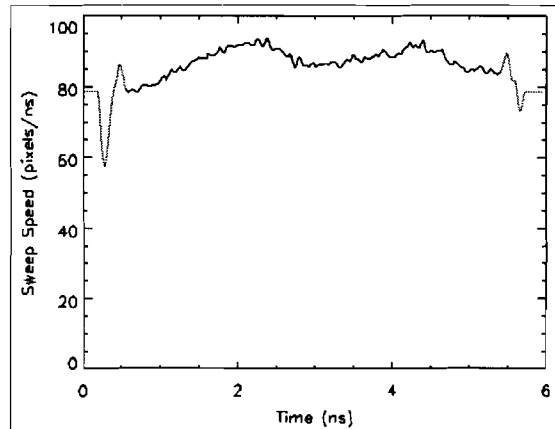

Figure 4

This image illustrates the problems inherent in the current sweep speed calibration routine. The portions .5 ns from the end oscillate wildly since no data is available for the interpolation. Also, high frequency noise is present along the entire sweep due to interpolation errors.

interpolation routine introduces high frequency noise into the data (see fig. 6).[4] The model created in this project will replace the spline interpolation, thus adding the ability to extrapolate beyond where data is collected and eliminating the noise problem.

The circuitry which generates the voltage ramp across the sweep plates was also developed at LLE. These sweep modules have a number of major features. The voltage pulse originates in a MOSFET/avalanche transistor stack which outputs a short pulse a few nanoseconds long. The pulse then goes through a double π-filter which filters out high frequency oscillations from the signal.[5] This filter will be referred to in this paper as the "main sweep filter". The pulse then goes through another π-filter which sets the module's main resonance frequency
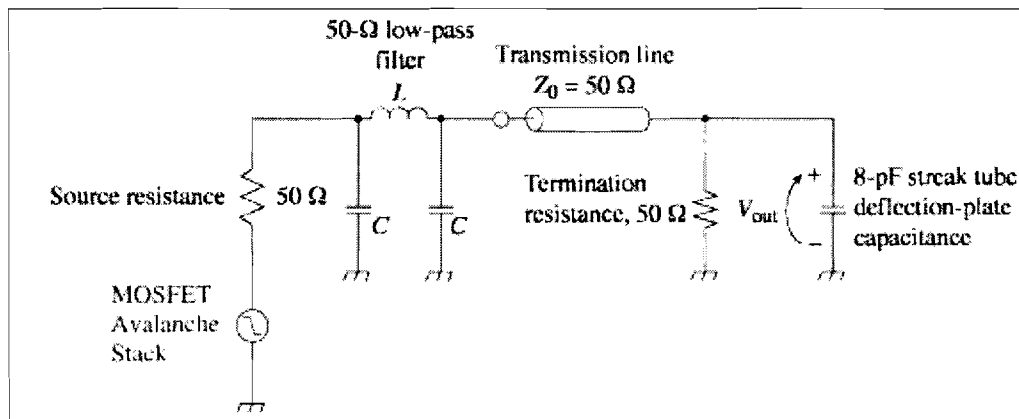

Figure 5

This is a simplified diagram of the circuitry which drives the sweep on P510 cameras. Please note that this simplifies the MOSFET and avalanche stacks, leaves out the π-filter, and does not note the parasitic components present in the circuit.

and thus the duration of the voltage ramp.[5] This filter will be referred to simply as the "π -filter". Finally, the signal is then sent through a transmission line to the sweep plates (see fig. 7). In addition to the components actually installed in the system, the wires connecting these components have parasitic inductances and capacitances associated with them. All the units used in P510 cameras at LLE are constructed identically.[5] There are, however, variations between units, particularly in the transistor stacks which provide the initial pulse.[4] As a result, certain characteristics of one unit may be slightly different or absent entirely from another.

One of these units is attached to each sweep plate. Thus the magnitude of the total voltage change across the plates is roughly twice that from one unit. In typical operation, the units are set to produce a voltage ramp approximately 20 ns long; however, only approximately 6 ns of the voltage ramp actually maps onto the image (see fig. 8).

Analyzing Voltage

In a P510 streak camera, the sweep speed is fundamentally related to the rate at which the voltage across the sweep plates changes. The mathematical relationship is as follows:

$$\frac{\partial V}{\partial t} = \frac{\partial V}{\partial x} \frac{\partial x}{\partial t} \qquad (1)$$

This equation basically means that the derivative of the voltage ramp with respect to time is equal to the sweep speed multiplied by the volts per pixel value of the camera (the amount the voltage must be changed to yield a deflection of one pixel). The volts per pixel value was found to be roughly constant at all points on the CCD for each camera. Comparison of the derivative of measured voltage and sweep speed data confirmed the relationship between the two (see fig. 9). The basic shapes were comparable, thus confirming that the voltage and sweep speed are in fact closely related. Unfortunately, the measured voltage data was not accurate enough to serve as the basis for sweep speed calibration. As a result of the extremely high voltages involved and the short duration of the voltage ramp, measuring the fine structure of the voltage ramp was impossible. Thus, building a suitably accurate model of the sweep speed from measured voltage data was not a viable option. Instead, quantitative analysis of the circuit was done using a simulation.

The sweep circuitry was simulated using Cadence Design System's PSPICE software. Setting up the simulation required making certain simplifications in the circuit and adding
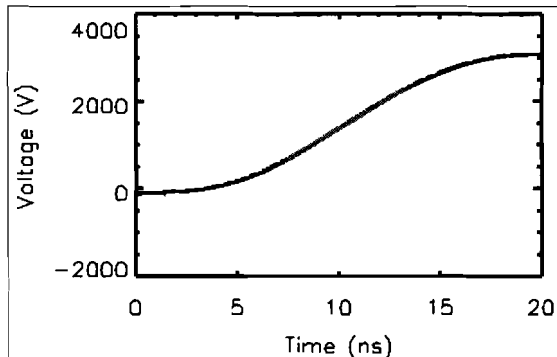

Figure 8

On any given sweep, only a small portion of the voltage ramp is used. In this case the sweep window is represented by the flat portion from 7 to 13 ns.
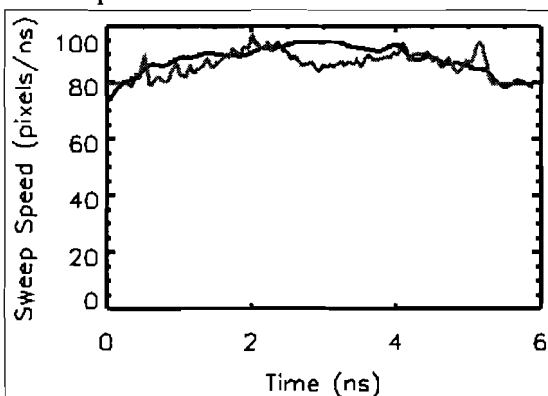

Figure 9

The jagged line represents sweep speed and smoother one the derivative of measured voltage data. This graph shows that their overall shapes are similar.

components not present in the actual circuit. First, the MOSFET and avalanche transistor stacks were approximated as piece-wise linear functions. This simplification captures the broad structure of the transistor stacks' output but may neglect certain finer structure. Moreover, considering that much of this fine structure varies from component to component, it could not be suitably modeled in the simulation. In addition, the circuit model included extra inductors and capacitors which compensated for the parasitic capacitive and inductive properties of the lengths of wire connecting the circuit's components.[6] The simulation's output was analyzed using tools built into the PSPICE software.

As a result of the inductive and capacitive elements in the circuit, the presence of certain resonant frequencies was assured. Three such frequencies were found by Fourier transforming the derivative of the voltage output. The part of the circuit creating that frequency was then found by measuring the oscillations across individual inductors and comparing that to the frequencies in the Fourier transform. The lowest frequency (38.62 MHz) was found to originate from the π-filter which sets the duration of the voltage ramp. This frequency had by far the highest amplitude, a logical outcome considering that this frequency is responsible for the broad structure of the entire voltage ramp. The second frequency (106.9 MHz) was linked to the main sweep filter. Finally, the third frequency (182.5 MHz) was found to be caused by the distributed parasitic inductive and capacitive components present in the circuit.

Creating a Model

These frequencies provided the basis for a model of the sweep speed. The initial model used three sine terms, each of which had a fixed frequency and two free parameters (a phase and an amplitude). It looked as follows:

$$\frac{\partial x}{\partial t} = A_\pi \sin(\omega_\pi t + \phi_\pi) + A_M \sin(\omega_M t + \phi_M) + A_P \sin(\omega_P t + \phi_P) \qquad (2)$$

The next step was to take this equation and fit it to sweep speed data. In order to ensure that the model would be useful over all possible sweep windows, it had to be fit over a time window longer than a single sweep. If this was not done, the model fit the peculiar structure of that particular sweep window and was inapplicable outside of it.

Creating this longer data set required some special work. First, five data sets of 30 images with varying trigger settings were taken from one of the P510's. While this data was somewhat less accurate than the usual 120 image calibration sets, it was sufficiently accurate for these purposes. Each of the five data sets represented a sweep speed generated from a different part of the voltage ramp. Once processed, this data was converted to a voltage (using equation 1) and compared to the measured output of the circuit. Although high-frequency structure is lacking in the measured voltage data, it still reflects the magnitude of the function at that point. As a result, one can use this relationship to correlate each sweep speed data set to a time interval on the voltage curve. This allows the relative temporal locations of the data sets to be determined. Once this is known, the five data sets can be combined into a single longer data set. Where sets overlapped, a weighted average was used giving greater weight to data points closer to the center of a data set.

Fitting the model to data was done in PV-WAVE with a non-linear regression routine which uses a modified Levenberg-Marquardt algorithm. The routine seeks to minimize the sum of the squares of the errors between the fit curve and the data, also called the error function. By evaluating the error function while varying the values of the parameters, the routine approximates the gradients of the error function in the parameter space. It uses these gradients to find the minimum of the error function, the location of best fit.[7]

Unfortunately, when this model was fit to data there were higher frequency elements that it could not explain (see fig. 10). While the model was able to explain the broad structure of the voltage ramp, two strong sinusoidal terms were still present in the residuals. This indicated that there were frequencies in the real circuitry that did not show up in the circuit simulations. The exact source of these oscillations is unknown; however, given the fact that the MOSFET/avalanche transistor stack was simplified in the circuit simulation, it is possible that it could produce certain frequencies which were not accounted for in the simulation. Moreover, since each camera uses two separate circuits to generate its sweep voltage, the frequencies may in fact emanate from two separate sweep drivers; however, determining the source of these residual frequencies with any certainty would require further investigation.

In order to create a workable model, two additional terms were added onto it. Each of these terms allowed the frequency to vary in addition to the amplitude and phase. The final model looked as follows:

$$\frac{\partial x}{\partial t} = A_\pi \sin(\omega_\pi t + \phi_\pi) + A_M \sin(\omega_M t + \phi_M) + A_P \sin(\omega_P t + \phi_P)$$
$$+ A_1 \sin(\omega_1 t + \phi_1) + A_2 \sin(\omega_2 t + \phi_2)$$

(3)

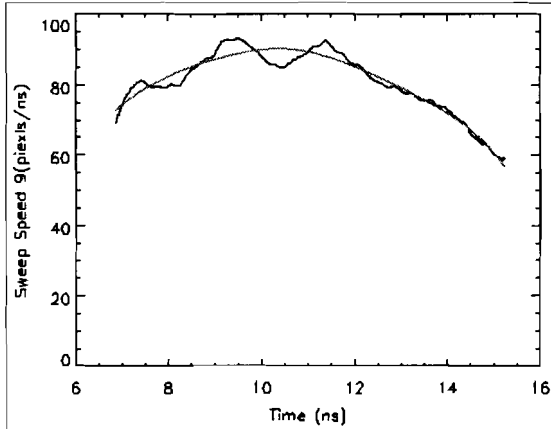This refined model led to a much better fit of the long data set (see fig. 11).

Figure 10

The smooth curve represents the three-term model while the oscillating curve represents the data. The three-term model fails to account for higher frequency structure in the real data.
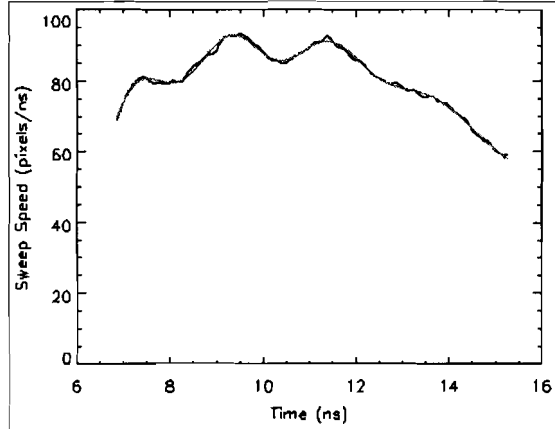

Figure 11

The smooth curve represents the five-term model and the more jagged curve represents the data. Using five-term produces a close correspondence to the measured sweep speed.

Once the model had been created, the uncertainties in each of the parameters were calculated. This was done using the following relationship:

$$\text{uncertainty in a} = \epsilon_a = \Delta a$$

where $X^2(a + \Delta a) = X^2(a) + 1$ and $X^2 = \sum \frac{(f(a) - y_i)^2}{\delta_i^2}$

(4)

By varying each parameter from its optimized position one at a time, values of the curve fit's chi-squared function were calculated around its minimum. An interpolation was then used to find where the chi-squared had increased by one from its value when the function was optimized. This change in the parameter was equal the standard deviation of that parameter. This process was repeated for each of the function's parameters.[8,9]

Parameter	A_π	ϕ_π	A_M	ϕ_M	A_P	ϕ_P
Value	$98.7\,px/ns$	$-1.12\,rad$	$13.8\,px/ns$	$3.33\,rad$	$3.24\,px/ns$	$-5.83\,rad$
Uncertainty (%)	±0.03	±0.04	±0.24	±0.07	±0.99	±0.17
Parameter	A_1	ω_1	ϕ_1	A_2	ω_2	ϕ_2
Value	$1.18\,px/ns$	$505\,MHz$	$-1.95\,rad$	$3.43\,px/ns$	$447\,MHz$	$.106\,rad$
Uncertainty (%)	±1.75	±0.05	±0.93	±0.92	±0.03	±9.01

The final step was to move to a shorter, single-sweep time window while maintaining the shape of the fit over the longer window. Doing this required that the term's phases and amplitudes be fixed relative to each other and that the two fit frequencies be fixed. The only parameters allowed to vary were the amplitude and phase of the π-filter term. All other phases were defined as a function of the π-filter phase in order to keep the terms in relative phase with each other no matter which time window was being examined. The other phases were defined as follows:

$$\phi_n{}' = \frac{\omega_n}{\omega_\pi}(\phi_\pi{}' - \phi_\pi) + \phi_n \tag{5}$$

Likewise, the ratios of the amplitudes were fixed. This allows the fit to adjust in instances where the voltage curve is simply dilated, the result of a change in the voltage applied to sweep circuitry. The relationship used here is shown below.

$$A_n{}' = A_\pi{}' \frac{A_n}{A_\pi} \tag{6}$$

This two-parameter curve fit weekly 120 image calibration data well (see fig. 12); however, now that the fit had been reduced to two parameters, it was not necessary to have the hundreds of data points which 120 images could provide. On each OMEGA system shot, there are eight fiducial pulses present on the top and bottom of the camera's output. Each set of eight pulses can be used to generate seven approximations of the sweep speed. When the sweep speed was fit to just one set of these fiducials (seven data points), the fit was nearly identical to that obtained from a 120 image, 700 data point data set (see fig. 13). Simply, this means that the
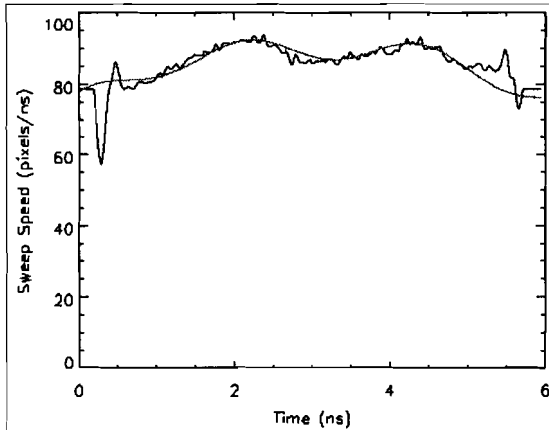

Figure 12

The model is represented by the smooth line and the measured sweep speed by the jagged line. The two-parameter model fits weekly, 120 image data well.
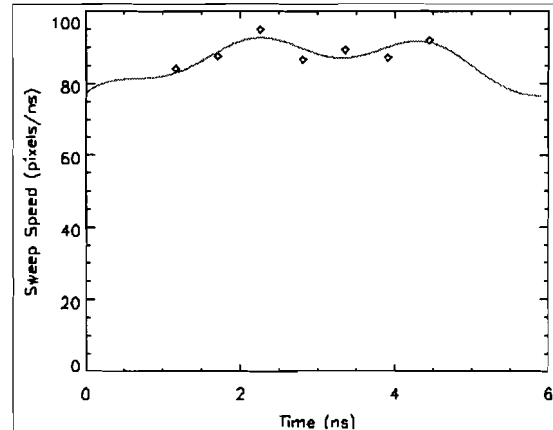

Figure 13

The model is represented by the line and the measured sweep data by the data points. The fit using a single image is very similar to the fit at left which uses 120 images.

sweep speed can be re-calibrated using the fiducial data in the event of malfunction.

Conclusion

Analysis of a streak camera's voltage module provides a suitable basis for a model of its sweep speed. This model will be useful in both better calibrating streak cameras on a weekly basis by avoiding the limitations of an interpolation routine and in recovering data in the event the cameras malfunction. Moreover, this work should be useful beyond the realm of P510 streak cameras. All streak cameras at LLE have fiducial lasers present; however, most cameras do not have weekly calibration procedures like the P510's and simply use the eight fiducial pulses to approximate the sweep speed at seven points during each shot. If a sweep speed model were constructed based on those cameras' circuitry, their calibrations and thus the accuracy of their output could be greatly enhanced.

Acknowledgments

I would like to thank Dr. Stephen Craxton, director of the Summer High School Research Program at LLE for giving me the opportunity to work at LLE during the summer of 2001. I would also like to thank Mr. Robert Boni for his help in collecting data from the P510's, Mr. Wade Bittle for creating the circuit model used in this project, and Dr. James Knauer for help regarding error analysis. Finally, I would like to thank my advisor, Dr. William Donaldson for all the time and help he gave me. There is no question that this project would have been impossible without him.

References

1. R. A. Lerche, D. S. Montgomery and J. D. Wiedwald, "High Contrast Ratio Power Measurements with a Streak Camera" SPIE 1539 68 (1991).

2. T. R. Boehly, R. S. Craxton, T. H. Hinterman, P. A. Jaanimagi, J. H. Kelly, T. J. Kessler, R. L. Kremens, S. A. Kumpan, S. A. Letzring, R. L. McCrory, S. F. B. Morse, W. Seka, S. Skupsky, J. M. Sources, and C. P. Verdon, "The upgrade to the OMEGA laser system," *Fusion Technol.* **26**, 722-729 (1994).

3. W. R. Donaldson, R. Boni, R. L. Keck, and P. A. Jaanimagi, "Self-Calibrating, Multichannel, Streak Cameras for Inertial Confinement Fusion Applications," to be published in Review of Scientific Instruments.

4. W. R. Donaldson (private communication).

5. "Design and Performance of a Selectable-Rate Streak-Camera Deflection Ramp Generator," *Laboratory for Laser Energetics LLE Review* **85**, 21-28.

6. W. Bittle (private communication).

7. PV-WAVE Advantage Reference. (Visual Numerics, Houston, 1993), p. 485-494.

8. P. R. Bevington, Data Reduction and Error Analysis for the Physical Sciences. (McGraw-Hill, New York, 1969), p. 242-243.

9. J. Knauer (private communication).